

# RESERVOIR MODELLING AND SIMULATION: INITIAL APPROACH FOR CO<sub>2</sub> STORAGE CAPACITY ESTIMATION IN IRATI FORMATION, PARANÁ SEDIMENTARY BASIN

*Nathalia Weber*

### ABSTRACT

With the production increase of its energy resources in the last decade, shale gas reservoirs have become an object of a technical feasibility study for geological carbon storage projects. In Brazil, Irati Formation stands out for its high potential for natural gas generation and its strategic location in the Paraná Basin due to its proximity to regions with higher concentrations of stationary carbon dioxide (CO<sub>2</sub>) emission sources. For initial estimates of the CO<sub>2</sub> storage potential in this geological formation, this chapter presents the results of reservoir modelling and numerical simulations for an injector well project with a geological model based on Irati. For a geological unit with dimensions of 1,200 m X 600 m X 40 m, the storage capacity results are close to 800,000 tons of CO<sub>2</sub>, considering established safety parameters. The sensitivity analysis as a function of the maximization of the injection indicated the most significant influence of the reservoir's pressure, thickness, and gas saturation for this evaluation.

**Keywords:** Geological Carbon Storage; Unconventional Reservoirs; Numerical Reservoir Simulation.

## 1. INTRODUCTION

Evaluating CO<sub>2</sub> storage capacity and injectivity potential in deep geological formations can be performed by applying several estimation methods based mainly on porosity, fluid saturation in the pores, and depth. The use of numerical reservoir simulation software allows to include elements related to fluid dynamics and parameters of well engineering and operation of the injection process, among other benefits in the analysis.

Numerical reservoir simulation is one of the methods traditionally used in petroleum engineering to predict the behaviour of oil and gas reservoirs from numerical solutions. Generally, numerical reservoir or flow simulators use the formulation and solution of mathematical equations that describe physical processes through (i) the application of a set of fundamental laws, such as the mass conservation, energy conservation, and momentum conservation; (ii) the mathematical description of a transport phenomenon linked to the nature of the process; and (iii) the appropriate state equations (Rosa et al., 2006). With the introduction of information on geological data, rocks and fluids properties, and the production and completion method, numerical reservoir simulators are applied to analyse the reservoir's behaviour, determine the best field for a development scheme, and improve knowledge of the reservoir's geology, among other possibilities.

Several authors used numerical reservoir simulation for studies related to capacity, safety, and injection strategies for geological CO<sub>2</sub> storage, with higher frequency in saline aquifers. Studies focused on shale reservoirs as potential CO<sub>2</sub> receptors are significantly smaller in quantity, with few exceptions, based on advanced gas recovery processes due to the shale's preference of adsorption by CO<sub>2</sub> over methane (CH<sub>4</sub>). These studies cover feasibility analysis of CO<sub>2</sub> storage (Kalantari-Dahaghi, 2010; Zhan et al., 2017), comparisons of advanced recovery methods strategies (Eshkalak et al., 2014; Jiang et al., 2014; Kim et al., 2017), analysis of factors of influence on injection efficiency (Kim et al., 2017) and studies applied to specific geological regions/formations (Schepers et al., 2009; Liu et al., 2013; Liu et al., 2016). As a study focused exclusively on carbon storage, without considering gas production, Chen et al. (2015) estimate CO<sub>2</sub> storage capacity in a depleted shale gas reservoir, based on the New Albany Formation, with sensitivity analysis of storage capacity.

## 2. RELEVANT ASPECTS TO SHALE GAS RESERVOIRS MODELLING AND SIMULATION

Predicting shale gas reservoirs' behaviour by numerical simulation presents additional challenges for modelling the system in comparison to conventional reservoirs. Among other reasons, the order of magnitude of permeability stands out, varying from nano to microDarcy. In addition, the little experience with the production of these resources so far, compared to the experience with conventional ones, leads to the lack of empirical knowledge of these reservoirs' behaviour (Houzé et al., 2018).

Beyond the low permeability, the challenges of modelling unconventional reservoirs are the intricate flow geometry, the combination of transport processes and the strong interactions between rocks and fluids (Wu et al., 2014). The different gas transport mechanisms, such as non-Darcyan flow, Knudsen diffusion and adsorption/desorption processes, are caused by complex networks of natural shale fractures and geochemical properties, such as the gas storage mechanism by adsorption (Javadpour et al., 2007; Sun et al., 2013; Wu et al., 2014). The interaction between the reservoirs' natural fractures with the hydraulic fractures from the well contributes to this complexity and non-planarity (Cipolla et al., 2010).

Based on the raised concerns, the construction of a geological model for reservoir simulation should cover relevant aspects such as natural fracture networks, gas adsorption, and diffusion mechanisms. In addition, to maximize CO<sub>2</sub> injection, the model must consider a horizontal well with hydraulic fracturing due to the low vertical permeability characteristic of shale gas reservoirs.

## 3. METHODS

In the first group of activities, the main factors that influence the capacity of geological carbon storage were identified based on a literature review. This identification was engaged in defining geological characteristics and CO<sub>2</sub> injection parameters for the simulation. Due to the low exploitation activity in the targeted region of Irati Formation in Paraná Basin and the absence of production history in the Formation, it was necessary to complement geological data with another formation of black shales. The Barnett Formation in the United States of America was selected due to its use by the Brazilian National Agency for Petroleum, Natural Gas and Biofuels (ANP) as a reference for estimating the potential of Brazilian formations of black shales for hydrocarbons, in addition to the excellent availability

of information in the literature. In addition, other general parameters for known shale formations were considered in the model.

The geological base model (M0) was constructed in the Builder module of the Computer Modelling Group simulator (CMG-2017) and a horizontal well with hydraulic fractures. The CO<sub>2</sub> injection rate in this proposal is limited by the injection pressure, which respected the formation fracture pressure, assumed based on the fracture gradient of 16.97 kPa/m, referring to the median value between 11.31 kPa and 22.62 kPa estimated for shale formations by Halliburton (2008).

Numerical simulations were then performed in the Compositional Module GEM (Generalized Equation-of-State Model Compositional Reservoir Simulator) of CMG in 1,000 years to determine the total theoretical capacity of CO<sub>2</sub> injection. A sensitivity analysis was performed with the maximization of CO<sub>2</sub> injection as an objective function to understand the influence of geological characteristics on capacity injection.

Due to geological uncertainties, pessimistic and optimistic boundary models were created, with minimum (M-) and maximum (M+) possible values of the main relevant characteristics to CO<sub>2</sub> storage capacity, based on estimated values from other black shale formations in the world. Variations in Irati Formation's porosity were also included in the boundary models. These models were then submitted to numerical simulation in GEM to obtain the range of results for theoretical CO<sub>2</sub> injection capacity potential.

### **3.1 Geological base model**

The three-dimensional base geological model (M0) was created in the Builder module of CMG, with an area of 1,200 m x 600 m, sufficient to safely incorporate the volume of influence of a horizontal injector well with hydraulic fracturing. The thickness was determined as 40 m, pointed out by Milani et al. (2007) as an average value for the Irati Formation. Due to the low permeability, CO<sub>2</sub> storage potential is restricted to the volume stimulated by the wells and the hydraulic fractures, allowing the analysis through reservoir simulation to be focused only on the influence of the injector well, considering no major faults in the region. The reservoir is initially composed only of CH<sub>4</sub> and water.

Generally, reservoirs with natural fractures are represented in a simplified form by double porosity, which classifies the values between matrix porosity and fractures to reduce the simulation time considerably. This simplification was adopted in this study, considering the presence of natural fractures in Irati. The approximated pore space in percentage was calculated concerning the total area of

Irati Formation's MEV images presented in De Souza (2018) for the matrix porosity. The base model's intermediate value of 6% was adopted, while the boundary models' porosity range of 4% and 8% was used. These numbers are within the field of average porosities of potential reservoirs of the known black shales in the world. The survey of porosities estimated in studies by the United States Energy Information Administration (EIA, 2011 and 2013), which evaluated recoverable hydrocarbon resources of shale formations in 137 formations worldwide, presented 1.6% to 12%. Due to the absence of data or reference for porosity calculation of the natural fractures of Irati, an average value found in 0.5% shales was adopted, pointed out in Wang and Reed (2009).

Two main conditions supported the determination of the depth for the base model the first concerns the physical state of CO<sub>2</sub> to be injected. To maximize the volume to be injected for storage, CO<sub>2</sub> must be in a supercritical state, i. e., at pressures and temperatures above 7.38 MPa and 31.1 °C, assuming more significant potential for compression. This point is reached at depths between 800 and 850 m (van der Meer, 2005; Holloway and Savage, 1993). It was also considered a safety margin of 1,000 m of distance from the Guarani Aquifer, which has an average depth of 320 m, according to 50 wells registered in the Hydrogeological Database of the extinct Water Resource Development Superintendence and Environmental Sanitation of the State of Paraná. Thus, the selected depth was 1,320 m, meeting the mentioned conditions. Although Irati Formation reaches the depth of 3,000 m, this value with more significant potential for CO<sub>2</sub> storage was chosen to expand the scope of this study.

Regarding reservoir pressure, an average hydrostatic pressure gradient of 0.475 psi/ft was assumed as used in Barnett (Vidas and Hugman, 2008). This number is not different from generally adopted mean values since EIA (2013) uses pressure gradients from 0.35 to 0.6 psi/ft depth – later used in the boundary models. Since 1 psi/ft is equivalent to 22,621 kPa/m, the reservoir of the base model with a 1,320 m depth was established at a pressure of 14,183 kPa.

Gomes (2010) brought results of geothermal resources of up to 64 °C for a depth of 1 km in the Paraná Basin. The temperature adopted was 49 °C based on a conservative approach. Permeability values, considered extremely low for shales, were extracted from Bhandari et al. (2015) with values for Barnett of 0.0000963 mD and 0.0000023 mD for horizontal and vertical permeabilities matrix, respectively. For the permeability of natural fractures, the value assumed was applied in reservoir numerical simulation in Zhu et al. (2017), based on Heller and Zoback (2014).

Given the absence of references for water saturation to the determined depth, a 55% gas saturation was defined, and its impact was included in the later analyses. The relevant aspects for shale gas reservoir modelling observed in the theoretical survey of the present study – a network of natural fractures, adsorption, and diffusion mechanisms – were also incorporated into the models used for a simplified representation of Irati. The networks of natural fractures were integrated using a model with double porosity, distinguishing porosities and permeabilities between matrix and fracture, whose values have already been treated in this description of the method.

The Langmuir parameters from Weniger et al. (2010) analysed isotherms of samples from the Irati Formation were adopted. For this base model, the results of sample 08\_170 were adopted since it represents intermediate values. Converting the pressure numbers from MPa to kPa-1 and maintaining the importance of substance quantity (mmol/g equal to gmol/kg), it was obtained for CH<sub>4</sub> Langmuir pressure and volume equivalent to 0.25 gmol/kg and 7.062x10<sup>-5</sup> kPa-1 and, for CO<sub>2</sub>, 1.25 gmol/kg and 7.45x10<sup>-5</sup> kPa-1.

Incorporating diffusion mechanisms based on the nanometric scale was considered a non-darcy flow and constant diffusion coefficients for CH<sub>4</sub> and CO<sub>2</sub>. The CH<sub>4</sub> and CO<sub>2</sub> diffusion coefficients analysis in Wang et al. (2017) showed variations from 1.4x10<sup>-7</sup> to 1.6x10<sup>-6</sup> cm<sup>2</sup>/s. Another considered point was the difference between the two values. The diffusion coefficient of CO<sub>2</sub> is lower than CH<sub>4</sub> under the same pressure (Wang et al., 2017). Thus, the values determined were 1.0x10<sup>-6</sup> and 0.8x10<sup>-6</sup> for CH<sub>4</sub> and CO<sub>2</sub>, respectively.

Finally, other essential characteristics for shale gas reservoirs behaviour analysis were added to the model, based on assumptions from reservoir simulation studies in shale formations, (i) density, assumed at 2,550 kg/m<sup>3</sup> by Aguilera (2016) for the Barnett, Marcellus, and Haynesville Formations; and (ii) matrix compressibility, established at 4.4x10<sup>-7</sup> in simulation for Yu et al. Fm. Barnett (2014). Table 1 presents a summary of the data used in the construction of the M0 base model.

<b>Feature</b>	<b>Value</b>	<b>Reference</b>
Dimensions (m)	1,200 x 600 x 40	(a)
The porosity of the matrix (fraction)	6%	De Souza (2018) <sup>1</sup>
Porosity of natural fractures (fraction)	0,5%	Wang and Reed (2009)

Horizontal matrix permeability (nD)	96,3	Bhandari et al. (2015)
Vertical matrix permeability (nD)	2,3	Bhandari et al. (2015)
Permeability of natural fractures (MD)	0,01	Zhu et al (2017) and Heller and Zoback (2014)
Depth (m)	1.320	(b)
Pressure (kPa)	14.183	(c)
Temperature (°C)	49	Gomes (2010) <sup>1</sup>
Initial gas saturation (fraction)	55%	Aguilera (2016)
Langmuir CH <sub>4</sub> volume (gmol/kg)	0,25	Weniger et al. (2010)
Langmuir CH <sub>4</sub> pressure (kPa-1)	7.06215x10 <sup>-5</sup>	Weniger et al. (2010)
Langmuir CO <sub>2</sub> volume (gmol/kg)	1,25	Weniger et al. (2010)
Langmuir CO <sub>2</sub> pressure (kPa-1)	7.45x10 <sup>-5</sup>	Weniger et al. (2010)
Diffusion coefficient CH <sub>4</sub> (cm <sup>2</sup> /s)	1x10 <sup>-6</sup>	Wang et al. (2017)
Diffusion coefficient CO <sub>2</sub> (cm <sup>2</sup> /s)	0.8x10 <sup>-6</sup>	Wang et al. (2017)
Compressibility (kPa-1)	4.4x10 <sup>-7</sup>	Yu et al. (2014)
Density (kg/m <sup>3</sup> )	2.550	Aguilera (2016)

Table 1. Values used for the m0 base model reservoir.

<sup>1</sup> Calculated values based on the references;

(a) Area of 1,200 m x 600 m based on the dimensions of the horizontal well with fractures and width of 40 m (from Milani et al., 2007);

(b) Respecting a minimum of 800 m depth and the safe distance from the aquifer;

(c) Calculated based on the pressure gradient of Vidas and Hugman (2008).

### 3.2. Injection well

In addition to the data selection from the reservoir's geological characteristics, it was also included definitions of parameters related to the injector well engineering.

The well length and hydraulic fracturing stages density were established based on the example of wells with more recent completions used in Barnett, applied by

EIA (2013) as a reference to establish well stimulation parameters for estimating recovery factors. It was modelled a horizontal well (90°) with 1,000 m of extension and 11 stages of hydraulic fractures. The fractures' wing reaches 140 m, and the inner thickness is 0.6096 m (standard GEM value). The fractures' height was set at 10 m above and below the well, leaving a safety margin to not cover the total 40 m reservoir's thickness.

The determination of the potentially more critical item of the project, the bottom pressure of the well, is related to the formation's stress fracture pressure, which, by safety, should be higher than the total pressure of the reservoir during and after the end of the CO<sub>2</sub> injection period. Injection pressure is also the main factor that limits the injection rate. In a review of CO<sub>2</sub> injection studies in depleted shale gas reservoirs, Du and Nojabaei (2019) report definitions of injection rate restriction between 100 and 5000 Mscf/d, the same as 2,832 283,168 m<sup>3</sup>/d. However, these studies seek to determine the rate limit to maximize enhanced oil or gas recovery, which tends to result in lower injection rates when compared to the injection proposal specifically for CO<sub>2</sub> storage. Hoteit et al. (2019) use injection rate limits between 15 and 50,000 Mscf/d (424,753 and 1,415,842 m<sup>3</sup>/d) for CO<sub>2</sub> injection analysis exclusively for storage. For injection in non-depleted reservoirs, it is possible to establish a parallel with studies of saline aquifers since depleted hydrocarbon reservoirs are traditionally studied and targeted for CO<sub>2</sub> injection. Generally, the CO<sub>2</sub> injection rate for saline aquifers is limited by injection pressure, which respects the formation fracture pressure (Szulczewski, 2009). This approach can be considered conservative if one believes that the spread of fractures can benefit storage capacity, although it can be a reasonable parameter considering storage security.

For the calculation of fracture pressure, due to the absence of studies with this purpose at Irati, an average fracture gradient for shale formations was considered, ranging from 0.5 to 1.0 psi/ft (11.31 to 22.62 kPa/m) (Halliburton, 2008). These values were then considered for the boundary models, while the mean value of 0.75 psi/ft (16.97 kPa/m) was selected for the base model. Therefore, multiplying this gradient by the depth determined in the previously mentioned (1,320 m), a fracture pressure of 990 psi was obtained, equivalent to 22,395 kPa. The related condition between calculated fracture pressure and the original reservoir pressure is parallel to the associated requirements of Zhao et al. (2018) and Wanniarachchi et al. (2017). In the first analysis involving the impact of depleting shale gas reservoirs on fracture pressure, fracture pressures are 10% to 80% higher than the initial reservoir pressures, considering possible anisotropies of geomechanical

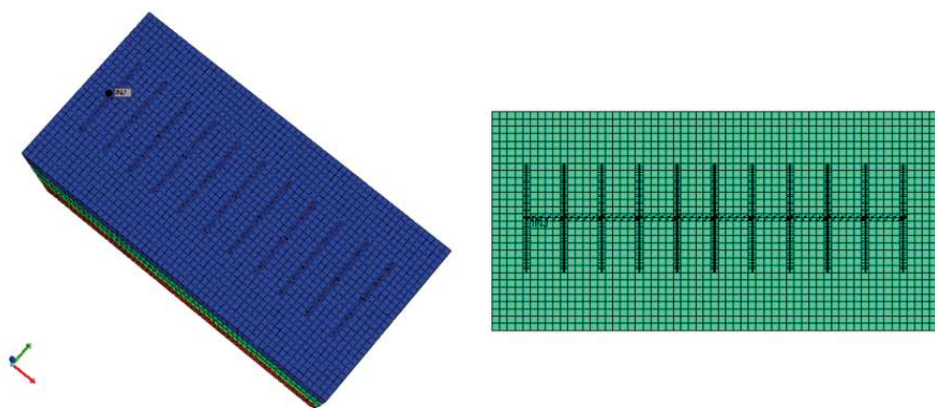


parameters. In Wanniarachchi et al. (2017), this proportion reaches up to 160%. Thus, the calculated value for fracture pressure considering a hypothetical reservoir of the Irati Formation is within this range, with a ratio of 60%. This comparison and identification of compatible values with studies in other formations is an essential indication of the choice of conservative and adequate numbers since this parameter – fracture pressure – has a significant impact on the potential for CO<sub>2</sub> storage capacity. Finally, considering a safety margin of 1,000 kPa, the well bottom hole pressure was set to 21,395 kPa for the base model.

Table 2 summarizes the values assumed for the well included in the base model, and Figure 1 displays images of the model on Builder.

Feature	Value
Well length (m)	1.000
Number of stages of hydraulic fracturing	11
Wings of fractures (m)	140
Internal thickness of fractures (m)	0,6096
Height of fractures (m)	20
Maximum pressure on well bottom (kPa)	21.395

Table 2. Values used for the injection well with hydraulic fracturing of the M0 base model.



1. Image of model M0, referring to the hypothetical reservoir in Irati and two-dimensional layer view with the well, in builder

### 3.3. Parameters for sensitivity analysis

The study involves the influence of the geological characteristics of the reservoir on CO<sub>2</sub> storage capacity. Since this is a relatively new approach, few studies

have this purpose applied to shale reservoirs. It is possible to establish parallels with essential factors in evaluating hydrocarbon accumulations in conventional reservoirs, such as porosity, permeability, and pressure. However, because these are unconventional reservoirs, we also consider volume stimulation by hydraulic fracturing and geochemical properties, notably the ability to adsorb CO<sub>2</sub> on the organic matter.

To contribute to the knowledge of unconventional reservoirs' behaviour as potential CO<sub>2</sub> storage units, a sensitivity analysis of geological characteristics was performed according to the maximization of the CO<sub>2</sub> injection volume. Thickness, porosity, permeability, pressure, temperature, initial gas saturation, CO<sub>2</sub> diffusion coefficient, compressibility, and rock density were varied in 20%, considering ten (10) years of injection. Pressure variations followed proportionally by variations in well bottom hole pressure, and 60% higher.

### **3.4 Geological boundary models**

Considering the geological uncertainties of the base model M0, the boundary models were also used in the simulations. It considers the minimum (M-) and maximum (M+) values based on other formations of black shale reservoirs worldwide. For this analysis of the potential range of CO<sub>2</sub> storage capacity of the Irati Formation, the following characteristics were varied from the base model (M0):

- Porosity, according to the estimated values Irati, from 4% to 8% (based on De Souza, 2018);
- Permeability, based on the maximum variation assumed in EIA (2013), from 0.00001 to 0.001 mD;
- Pressure, with variations in pressure gradients, assumed in EIA (2013) for sub pressure of 0.35 psi/ft and overpressure of 0.6 psi/ft, applied to a depth of 1320 m;
- Due to the difficulty to find values for water saturation in the literature, initial gas saturation was set at the values calculated in Aguilera (2016) for the Barnett, Marcellus and Haynesville formations, ranging from 35% to 45%, with safety margin, resulting in 30% to 50%;
- Langmuir parameters were extracted from Weniger et al. (2010) for the Irati Formation, with samples 08\_168 and 08\_154. The pessimistic model was set to 0.04 gmol/kg and pressure of  $1.77 \times 10^{-4}$  kPa-1 for CH<sub>4</sub> and 0.65 gmol/kg and  $5.03 \times 10^{-5}$  kPa-1 for CO<sub>2</sub>. The optimistic, with 0.37 gmol/kg and  $1.19 \times 10^{-4}$  kPa-1 for CH<sub>4</sub> and 2.02 gmol/kg and  $6.67 \times 10^{-5}$  kPa-1 for CO<sub>2</sub>;

- Rock bottom pressure, following the same reasoning established for M0, with fracture gradients ranging from 0.5 to 1.0 psi/ft (Halliburton, 2008).

Table 3 presents the values used in the construction of the boundary models.

Variable	M-	Base	M+	Reference
Porosity (fraction)	4%	6%	8%	Dias (2018) <sup>1</sup>
Permeability (mD)	0,00001	0,0000963	0,001	EIA (2013)
Pressure (kPa)	10.451	14.183	17.916	(a)
Gas saturation (fraction)	50%	55%	70%	Aguilera (2016)
Langmuir CH <sub>4</sub> volume (gmol/kg)	0,04	0,25	0,37	Weniger et al. (2010)
Langmuir CH <sub>4</sub> pressure (kPa-1)	1.77x10 <sup>-4</sup>	7.062x10 <sup>-5</sup>	1.19x10 <sup>-4</sup>	Weniger et al. (2010)
Langmuir CO <sub>2</sub> volume (gmol/kg)	0,65	1,25	2,02	Weniger et al. (2010)
Langmuir CO <sub>2</sub> pressure (kPa-1)	5.03x10 <sup>-5</sup>	7.45x10 <sup>-5</sup>	6.67x10 <sup>-5</sup>	Weniger et al. (2010)
Pressure at rock bottom (kPa)	13.930	21.395	28.860	(b)

Table 3. Definition of minimum and maximum values of geological characteristics for the composition of the M- and M+ boundary scenarios.

<sup>1</sup>Calculated based on the table reference.

(a) Calculated based on EIA pressure gradients (2013);

(b) Calculated based on the conditional relation between fracture pressure and training pressure.

## 4. RESULTS

The numerical reservoir simulation for a thousand years of the M0 base model indicated a theoretical potential of injection capacity of approximately 783,000 tons of CO<sub>2</sub>, as identified in Figure 2a. The total CO<sub>2</sub> injected annually starts with about 25,000 tons, with a decline of 47% in the first ten (10) years. From twenty years, the reduction is around 17% every ten years, with less stable variations after

260 years of injection. In the 136th year, the CO<sub>2</sub> injection rate is already below 1,000 tons per year and below ten tons in the 278th year of injection.

These results show that the injection time to achieve the total CO<sub>2</sub> storage capacity of the hypothetical reservoir exceeds the period of a commercial project since it seems unlikely to have a project with more than 136 years of planning. The injection rate was within the established parameter limits in other CO<sub>2</sub> injection studies in shale gas and oil reservoirs, reviewed in Du and Nojabaei (2019), peaking at 35,000 m<sup>3</sup>/d in the first year. The injection rate behaviour is presented in Figures 2d and 2e for 1,000 and 20 years injection time, respectively.

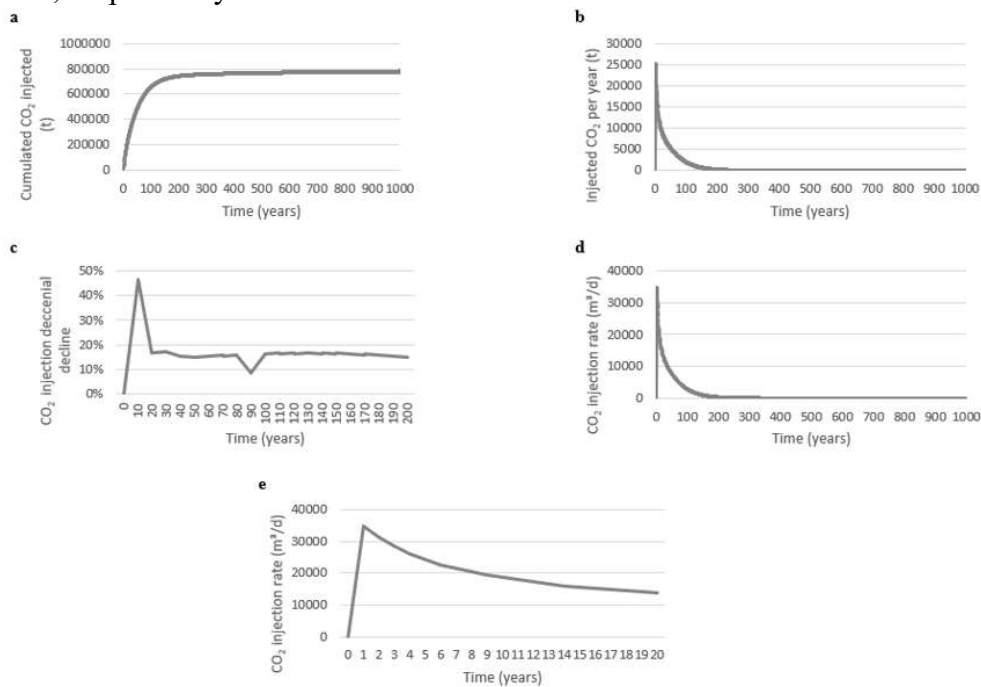


Figure 2. Simulation results for 1,000 years of injection to evaluate storage capacity: (a) accumulated CO<sub>2</sub> injected; (b) CO<sub>2</sub> injected per year; (c) decennial decline of CO<sub>2</sub> injection; (e) CO<sub>2</sub> injection rate.

Figure 3 shows the CO<sub>2</sub> proportion evolution in the gas phase in the four layers of the reservoir, each with 10 m. From “layer 1”, the CO<sub>2</sub> fraction is kept almost evenly between 20% and 30% at the end of the injection period. However, the small portions related to the upper part of the injector well passage and hydraulic fractures, the fraction can reach 60% of the gas phase. The same percentages stand in layer 2, where the well is located, but with the

regions around the well reaching more blocks. The third layer (top to bottom) has almost homogeneous proportions of 20% to 30% of CO<sub>2</sub>.

On the other hand, the last layer brings an entirely different pattern of CO<sub>2</sub> distribution concerning the total gas phase. The region around the well and hydraulic fractures with the highest CO<sub>2</sub> fraction occupies the entire area virtually, with values around 30% to 70%, leaving only the extremities with percentages from 0 to 20%. The higher water saturation can justify this behaviour concerning the other upper layers and, therefore, by the presence of extremely low amounts of CH<sub>4</sub>. Considering the low compressibility of water, the injected CO<sub>2</sub> that reached the fourth layer was entirely stored under the adsorbed phase.

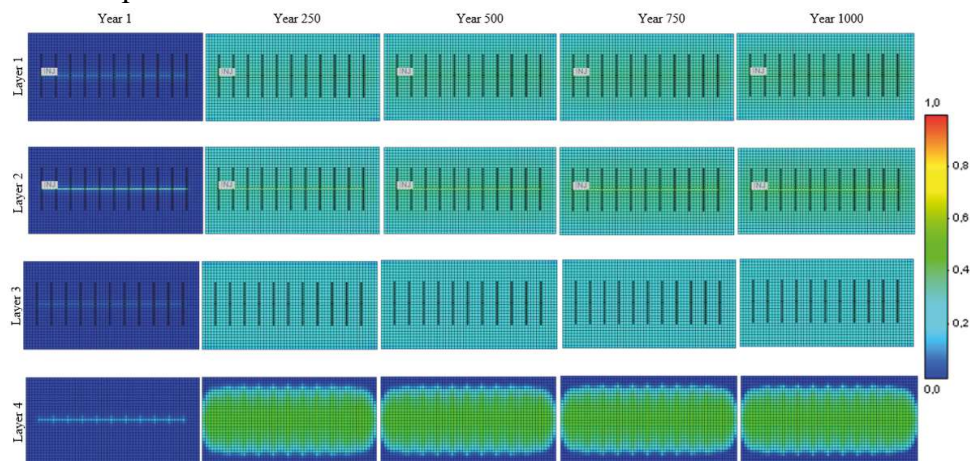


Figure 3. Plan view of the reservoir in four layers, identifying the evolution of the CO<sub>2</sub> fraction in the gas phase, up to the end of the CO<sub>2</sub> injection period, in selected years.

At the end of the injection period, the CO<sub>2</sub> adsorbed phase concerning the total stored ranged from 70% to 80% in the two upper layers and 80% up to 100% in the lower layers(Figure 4). Figure 5 shows the evolution of CO<sub>2</sub> adsorption in gmole/m<sup>3</sup> in the injector well layer until year 136, in which the injection flow was less than 1,000 tons of CO<sub>2</sub> per year.

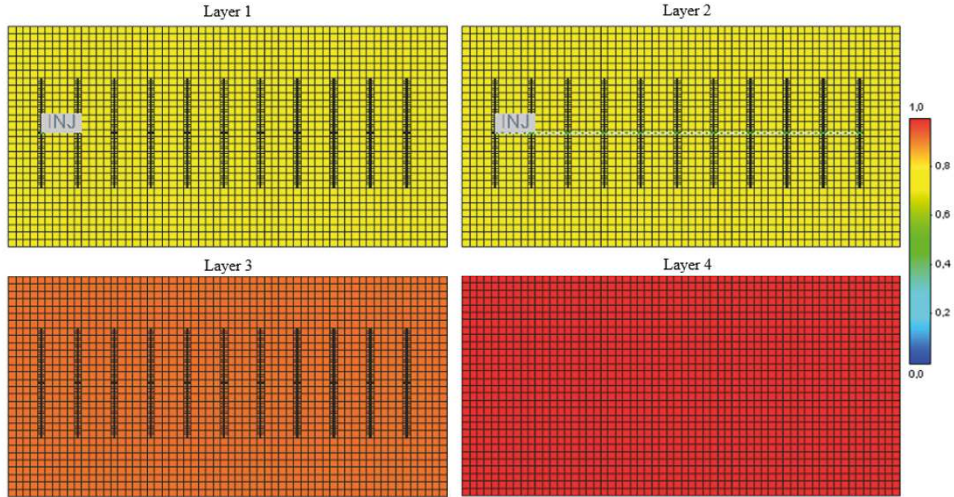


Figure 4. Plan view of the four layers of the reservoir at the end of the injection period,

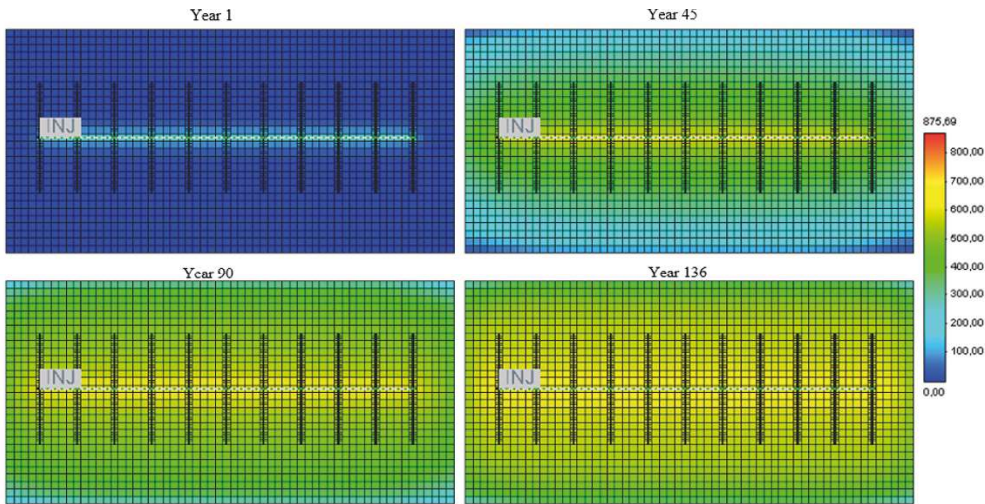


Figure 5. Plan view of layer 2, where the injector well is located, identifying the concentrations of CO<sub>2</sub> by volume, in gmole/m<sup>3</sup>, in selected years, up to the 136th year.

The total effectiveness of CO<sub>2</sub> storage in the adsorption phase presented 40% to 77%, as observed in Figure 6. At the end of the simulation period, approximately 13.68x10<sup>9</sup> CO<sub>2</sub> gmole were adsorbed, and 0.92x10<sup>9</sup> CH<sub>4</sub> gmole underwent a desorption process. However, it is impossible to establish a CO<sub>2</sub>/CH<sub>4</sub> displacement ratio, as it is unknown whether CH<sub>4</sub> reached the maximum adsorption potential before CO<sub>2</sub> injection was initiated.

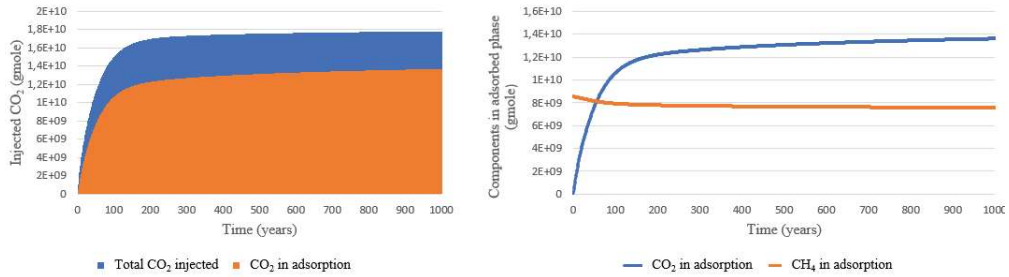


Figure 6. Evolution of the CO<sub>2</sub> in adsorption based on the total injected and CH<sub>4</sub> in adsorption in the reservoir, in M0.

The sensitivity analysis of the reservoir properties concerning CO<sub>2</sub> injection capacity indicated the most significant influence involving pressure, thickness, gas saturation, density, porosity, and permeability, in that order based on the results. The temperature, compressibility and CO<sub>2</sub> diffusion coefficient showed little influence, as shown in Figure 7. The variation of the reservoir pressure had more expressive results due to its established relationships with the variation of the injection pressure.

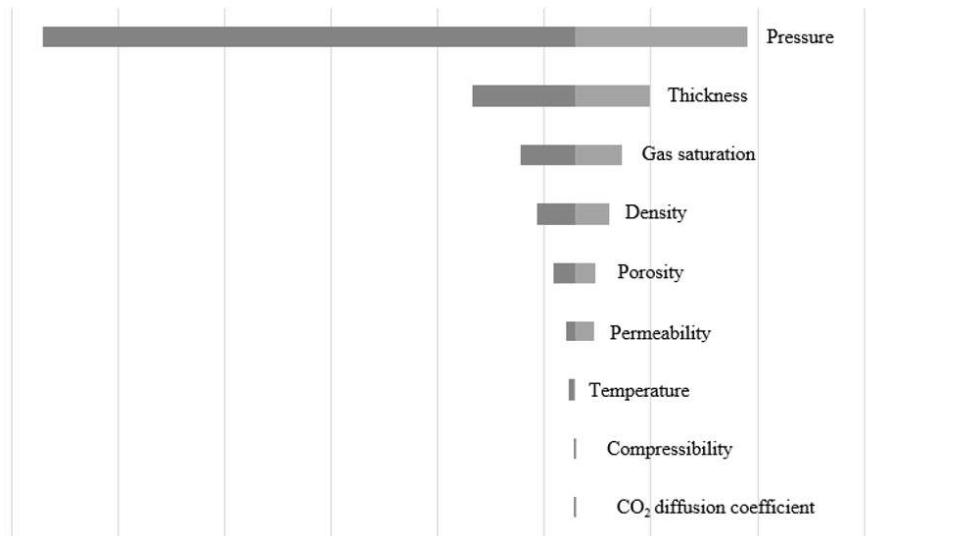


Figure 7. Sensitivity analysis of reservoir properties concerning CO<sub>2</sub> injection considering; pressure, thickness, gas saturation, density, porosity, permeability, temperature, compressibility, and CO<sub>2</sub> diffusion coefficient.

Storage safety was not impaired; the final reservoir pressure stayed below the fracture pressure. Only in the year 760, the reservoir reaches the value equivalent to the final pressure with the total CO<sub>2</sub> injected, 21,507 kPa, as identified in Figure 8.

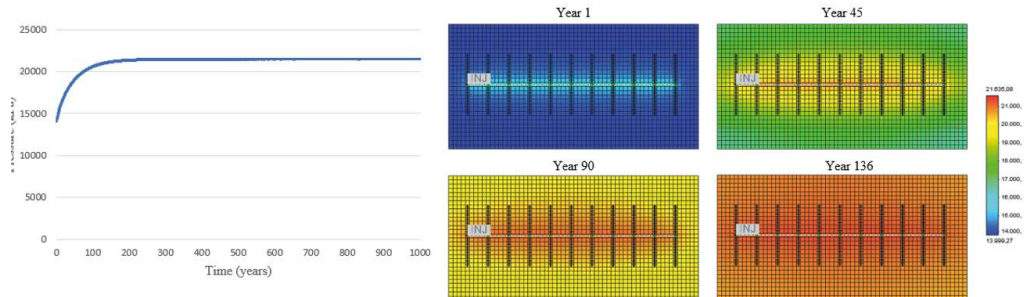


Figure 8: Evolution of pressure in the injection period, with a maximum value of 21,507 kPa reached in the year 760 and plan view of the layer with the well showing the evolution of pressure (in kPa) in selected years, in M0.

Regarding the simulations' results for M- and M+ boundary models, storage capacity was found between 166,000 and 1193,000 tons of CO<sub>2</sub>, demonstrating the extent of the impact of characteristic geological variations on the result when considered a virtually unrestricted injection time. Results for storage capacity and final CO<sub>2</sub> storage percentages in the adsorbed phase of 56% in M- and 69% in M+ are shown in Figure 9.

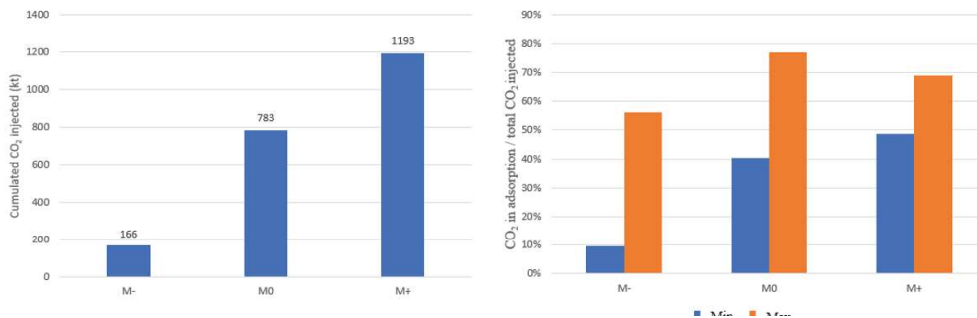


Figure 9. Comparison of CO<sub>2</sub> stored in the boundary models (M- and M+) and base model (M0), and comparison of the effectiveness of CO<sub>2</sub> storage in the adsorbed phase concerning the total injected, in the boundary models (M- and M+) and base model (M0), in 1000 years.

The capacity intervals between the pessimistic and optimistic scenarios demonstrate the significant influence of the variation of the reservoir properties, notably the pressure and gas saturation, since the thickness and density were not altered concerning the base model. Therefore, the relevance of obtaining refined data to construct the geological model is clear, reducing uncertainties. Assessing the total potential of the Irati Formation for CO<sub>2</sub> storage requires further studies to provide the entire area in which CO<sub>2</sub> injection activities can be carried out, considering the adequate spacing between wells. Because the thickness used in the model is the



average of the entire formation, the determined area would be multiplied by the results of this work, providing an estimate for the whole length of the Irati Formation.

The comparison of this potential with other shale formations is limited by the differences in literature approaches to date. In general, the CO<sub>2</sub> injection in shale gas reservoirs is studied for reservoirs that have already been the target of production and are almost always associated with enhanced recovery. If, on the one hand, storage capacity tends to be lower in non-depleted reservoirs, on the other hand, the objective of enhanced recovery tends to minimize CO<sub>2</sub> injection.

Despite the uncertainties of the applied parameters, the present study indicates estimates for the potential of CO<sub>2</sub> storage capacity in Irati without considering oil or gas production, based on the possibility of CO<sub>2</sub> injection up to a safety pressure lower than the reservoir fracture pressure. From this concept, the possibility of storing carbon in shale gas reservoirs is raised without the need for local production of fossil fuel resources.

## 5. CONCLUSIONS

The present study aimed to estimate the geological CO<sub>2</sub> storage capacity of Irati Formation in the Paraná Basin by a unit of geological volume based on numerical reservoir simulations. Essential characteristics were incorporated into the geological modelling of the shale gas reservoirs, such as a network of natural fractures, gas diffusivity, adsorption and hydraulic fracturing. The CO<sub>2</sub> injection pressure was limited to stay lower than the assumed formation's fracture pressure, with a injection period of 1,000 years, allowing it to reach the total theoretical storage capacity. The project was restricted to an injector well in a reservoir representative volume comprising the horizontal well extension with hydraulic fracturing, covering an area of 1,200 m for 600 m, with a thickness of 40 m.

The simulation results presented a capacity of 783,000 tons of CO<sub>2</sub>. The values may fluctuate between 166,000 and 1,193,000 tons, considering the pessimistic and optimistic scenarios of the reservoir properties. 77% of the injected CO<sub>2</sub> was stored in the adsorbed phase at the end of the injection period. The sensitivity analysis indicated the reservoir's pressure and thickness as factors of more significant influence on total capacity, followed by gas saturation and formation density.

The presented results and methodologies may serve as references to predict CO<sub>2</sub> injection and storage in other areas where the depth and thicknesses are close to those showcased by this study.

## ACKNOWLEDGEMENT

We are grateful for the support of FAPESP and Shell through the Research Centre for Gas Innovation - RCGI, organized by the University of São Paulo (USP), and the strategic importance of the support granted by the ANP through the R&D clause. We also thank the Institute of Energy and Environment of USP for hosting the research and CAPES and FUSP for the financial support.

## REFERENCES

- Aguilera, R. (2016). Shale gas reservoirs: Theoretical, practical and research issues. *Petroleum Research*, 1(1), 10–26. [https://doi.org/10.1016/s2096-2495\(17\)30027-3](https://doi.org/10.1016/s2096-2495(17)30027-3).
- Bhandari, A. R., Flemings, P. B., Polito, P. J., Cronin, M. B. & Bryant, S. L. (2015). Anisotropy and Stress Dependence of Permeability in the Barnett Shale. *Transport in Porous Media*, 108(2), 393–411. <https://doi.org/10.1007/s11242-015-0482-0>.
- Chen, Z., Liao, X., Zhao, X., Lv, S., Dou, X., Guo, X., Li, L. & Zang, J. (2015). Development of a Trilinear Flow Model for Carbon Sequestration in Depleted Shale. Society of Petroleum Engineers, October. doi:10.2118/176153-MS.
- Cipolla, C. L., Lolon, E. P., Erdle, J. C. & Rubin, B. (2010). Reservoir modeling in shale-gas reservoirs. *SPE Reservoir Evaluation and Engineering*, 13(4), 638–653. <https://doi.org/10.2118/125530-PA>.
- de Souza, J. D. (2018). Efeitos da composição mineralógica no potencial de Adsorção de gases (CO<sub>2</sub>/CH<sub>4</sub>) de folhelhos da Formação Irati: Implicações para caracterização de reservatórios Geológicos para armazenamento de CO<sub>2</sub>. Bachelor's thesis. Instituto de Geociências, Universidade de São Paulo, São Paulo.
- Du, F. & Nojabaei, B. (2019). A review of gas injection in shale reservoirs: Enhanced Oil/Gas recovery approaches and greenhouse gas control. *Energies*, 12(12). <https://doi.org/10.3390/en12122355>.
- EIA – United States Energy Information Administration. (2011). Review of Emerging Resources: U. S. Shale Gas and Shale Oil Plays. U. S. Energy Information Administration, July, 105 pp. Retrieved from: <<https://www.eia.gov/analysis/studies/usshalegas/pdf/usshaleplays.pdf>>.
- EIA – United States Energy Information Administration. (2013). Shale Oil and Shale Gas Resources: An Assessment of 137 Shale Formations in 41 Countries

Outside the US. June. Retrieved from: <<https://www.eia.gov/analysis/studies/worldshalegas/pdf/overview.pdf>>.

Eshkalak, M. O., Al-Shalabi, E. W., Sanaei, A., Aybar, U. & Sepehrnoori, K. (2014). EGR by CO<sub>2</sub> sequestration versus re-fracturing treatment in unconventional shale gas reservoirs. Society of Petroleum Engineers - 30th Abu Dhabi International Petroleum Exhibition and Conference, ADIPEC 2014: Challenges and Opportunities for the Next 30 Years, 6, 4107–4124. <https://doi.org/10.2118/172083-ms>.

Gomes, A. J. de L. Avaliação de recursos geotermiais da Bacia do Paraná. *Revista Brasileira de Geofísica*, 28(4), 745–745, 2010. <https://doi.org/10.1590/s0102-261x2010000400018>.

Halliburton (2008). Halliburton Hydraulic Fracturing: Over 60 Years of Successful Performance Focused on the Environment. Retrieved from: <[https://www.halliburton.com/content/dam/ps/public/pe/contents/Data\\_Sheets/web/H/H06640.pdf](https://www.halliburton.com/content/dam/ps/public/pe/contents/Data_Sheets/web/H/H06640.pdf)>.

Heller, R. & Zoback, M. (2014). Adsorption of methane and carbon dioxide on gas shale and pure mineral samples. *Journal of Unconventional Oil and Gas Resources*, 8(C), 14–24. <https://doi.org/10.1016/j.juogr.2014.06.001>.

Holloway and Savage. (1993). The potential for aquifer disposal of carbon dioxide in the UK. *Energy Conversion and Management*, vol 34, 9-11. Doi: 10.1016/0196-8904(93)90038-c.

Hoteit, H., Fahs, M., & Soltanian, M. R. (2019). Assessment of CO<sub>2</sub> injectivity during sequestration in depleted gas reservoirs. *Geosciences (Switzerland)*, 9(5), 1–19. <https://doi.org/10.3390/geosciences9050199>.

Houzé, O., Viturat, D. & Fjaere, O. S. (2018). Dynamic data analysis: the theory and practice of Pressure Transient Analysis, Rate Transient Analysis, Formation Testing, Production Logging and the use of Permanent Downhole Gauges. V5.20.02. KAPA. Retrieved from: <<https://www.kappaeng.com/documents/flip/dda520/files/assets/basic-html/page-1.html>> .

Javadpour, F., Fisher, D. & Unsworth, M. (2007). Nanoscale gas flow in shale gas sediments. *Journal of Canadian Petroleum Technology*, 46(10), 55–61. <https://doi.org/10.2118/07-10-06>.

Jiang, J., Shao, Y. & Younis, R. M. (2014). Development of a Multi-Continuum Multi-Component Model for EGR and CO<sub>2</sub> Storage in Fractured Shale Gas Reservoirs. Society of Petroleum Engineers. doi:10.2118/169114-MS.

- Kalantari-Dahaghi, A. (2010). Numerical simulation and modeling of EGR and CO<sub>2</sub> sequestration in shale gas reservoirs: A feasibility study. Society of Petroleum Engineers - SPE International Conference on CO<sub>2</sub> Capture, Storage, and Utilization 2010, 533–550. <https://doi.org/10.2118/139701-ms>.
- Kim, T. H., Cho, J. & Lee, K. S. (2017). Evaluation of CO<sub>2</sub> injection in shale gas reservoirs with multi-component transport and geomechanical effects. *Applied Energy*, 190, 1195–1206. <https://doi.org/10.1016/j.apenergy.2017.01.047>.
- Liu, D., Li, Y. & Agarwal, R. K. (2016). Numerical simulation of long-term storage of CO<sub>2</sub> in Yanchang shale reservoir of the Ordos basin in China. *Chemical Geology*, 440, 288–305.2016. <https://doi.org/10.1016/j.chemgeo.2016.08.002>.
- Liu, F., Ellett, K., Xiao, Y. & Rupp, J. A. (2013). Assessing the feasibility of CO<sub>2</sub> storage in the New Albany Shale (Devonian-Mississippian) with potential EGR using reservoir simulation. *International Journal of Greenhouse Gas Control*, 17, 111–126. <https://doi.org/10.1016/j.ijggc.2013.04.018>.
- Milani, E. J., Melo, J. H. G., Souza, P. A., Fernandes, L. A. & França, A. B. (2007). Bacia do Paraná. *Boletim de Geociências da Petrobras*, Rio de Janeiro, v. 15, n. 2, p. 265-287.
- Rosa, A., Carvalho, R. & Xavier, D. (2006). *Engenharia de Reservatórios de Petróleo*. 1 ed. Rio de Janeiro, Interciência,
- Schepers, K. C., Nuttall, B., Oudinot, A. Y. & Gonzalez, R. (2009). Reservoir modeling and simulation of the devonian gas shale of eastern Kentucky for EGR and CO<sub>2</sub> storage. SPE International Conference on CO<sub>2</sub> Capture, Storage, and Utilization 2009, 154–173. <https://doi.org/10.2118/126620-ms>.
- Sun, H., Yao, J., Gao, S., Fan, D., Wang, C. & Sun, Z. (2013). Numerical study of CO<sub>2</sub> enhanced natural gas recovery and sequestration in shale gas reservoirs. *International Journal of Greenhouse Gas Control*, 19, 406–419. <https://doi.org/10.1016/j.ijggc.2013.09.011>.
- Zulczewski, M. L. (2009). Storage Capacity and Injection Rate Estimates for CO<sub>2</sub> Sequestration in Deep Saline Aquifers in the Conterminous United States. Master's thesis. Department of Civil and Environmental Engineering. Massachusetts Institute of Technology.
- van der Meer, B. (2005). Carbon dioxide storage in natural gas reservoirs. *Oil and Gas Science and Technology*, 60(3), 527–536. <https://doi.org/10.2516/ogst:2005035>.

- Vidas, H. & Hugman, B. (2008). Availability, Economics, and Production Potential of North American Unconventional Natural Gas Supplies. Fairfax, Va. : The INGAA Foundation, November.
- Wang, F. P. & Reed, R. M. (2009). Pore Networks and Fluid Flow in Gas Shales. Society of Petroleum Engineers. doi:10.2118/124253-MS.
- Wang, Z., Li, Y., Liu, H., Zeng, F., Guo, P. & Jiang, W. (2017). Study on the adsorption, diffusion and permeation selectivity of shale gas in organics. *Energies*, 10(1), 1–15. <https://doi.org/10.3390/en10010142>.
- Wanniarachchi, W. A. M., Gamage, R. P., Perera, M. S. A., Rathnaweera, T. D., Gao, M. & Padmanabhan, E. (2017). Investigation of depth and injection pressure effects on breakdown pressure and fracture permeability of shale reservoirs: An experimental study. *Applied Sciences (Switzerland)*, 7(7). <https://doi.org/10.3390/app7070664>.
- Weniger, P., Kalkreuth, W., Busch, A. & Kross, B. M. (2010). High-pressure methane and carbon dioxide sorption on coal and shale samples from the Paraná Basin, Brazil. *International Journal of Coal Geology* 84,190–205.
- Wu, Y. S., Li, J., Ding, D. Y., Wang, C. & Di, Y. (2014). A generalized framework model for the simulation of gas production in unconventional gas reservoirs. *SPE Journal*, 19(5), 845–857. <https://doi.org/10.2118/163609-PA>.
- Yu, W., Al-Shalabi, E. W. & Sepehrnoori, K. (2014). A Sensitivity Study of Potential CO<sub>2</sub> Injection for EGR in Barnett Shale Reservoirs. *SPE Unconventional Resources Conference – USA*. <https://doi.org/10.2118/169012-MS>.
- Zhan, J., Yuan, Q., Fogwill, A., Cai, H., Hejazi, H., Chen, Z. & Cheng, S. (2017). A Systematic Reservoir Simulation Study on Assessing the Feasibility of CO<sub>2</sub> Sequestration in Shale Gas Reservoir with Potential EGR. *Carbon Management Technology Conference*.10.7122/484390-MS.
- Zhao, K., Yuan, J., Feng, Y., & Yan, C. (2018). A novel evaluation on fracture pressure in depleted shale gas reservoir. *Energy Science and Engineering*, 6(3), 201–216. <https://doi.org/10.1002/ese3.198>.
- Zhu, L., Liao, X., Chen, Z., Cheng, X. (2017). Performance evaluation for carbon sequestration in shale gas reservoir systems. *Carbon Management Technology Conference, CMTC 2017: Global CCUS Innovation Nexus*, 1, 183–197. <https://doi.org/10.7122/485740-ms>.

